Transactions of the Materials Research Society of Japan 29[4] 1293-1298 (2004)

Application of 60 mm-diameter Superconducting Bulk Magnet to Magnetron Sputtering

U.Mizutani, H.Hazama[1], T.Matsuda[2], Y.Yanagi[3], Y.Itoh[3], H.Ikuta, A.Imai[1], A.Sekiguchi[4] and K.Sakurai[4]

Department of Crystalline Materials Science, Nagoya University, Furo-cho, Chikusa-ku, Nagoya 464-8603, Japan
Fax: 81-52-789-3821, e-mail: mizutani@nuap.nagoya-u.ac.jp
[1]Nagoya Industrial Sci. Res. Inst., Anagahora, Shimoshidami, Moriyama-ku 463-0003, Japan
[2]DIAX Co., Ltd., 44 Chikoin, Shimoyashiki-cho, Kasugai 486-0909, Japan
[3]IMRA MATERIAL R&D Co., Ltd., 5-50 Hachiken-cho, Kariya 448-0021, Japan
[4] ANELVA CORP., 5-8-1 Yotsuya, Fuchu-shi, Tokyo 183-8508, Japan

The present planar-magnetron sputtering apparatus is activated by a c-axis oriented single-domain Sm123 superconducting bulk magnet of 60 mm in diameter. A magnetic field reaching 6.3 T at the surface of the superconductor coupled with a target voltage of max. 6 kV enabled us to discharge even at pressure of 3.3 x 10^{-3} Pa. The magnetic field with a vanishing z-component, $B_{//}^{max}$, reached 1.2 Tesla on the 1 mm thick Cu target. A target-to-substrate or throw distance can be set at 300-500 mm under low pressures of 10^{-2} to 10^{-3} Pa to form a sputtered film with reasonable deposition rates. The discharging characteristics of Cu, Ni, Al, Fe and C targets in the pressure range over 10^{-1} to 10^{-3} Pa were studied. The deposition rates of 0.1 nm/s (or 60 Å/min) and 0.025 nm/s (or 15 Å/min) were achieved for 3 mm thick Cu and Fe targets, respectively, under the Ar pressure of $6.6x10^{-2}$ Pa and throw distance D_{st}=300 mm. By taking full advantage of the uniqueness in the present magnetron sputtering, we could coat uniformly with Cu both bottom and sidewall of a via hole down to 200 nm in diameter without any overhang near its edge.

Key words: superconducting permanent magnet, magnetron sputtering, high vacuum deposition, bottom coverage of via hole

1. INTRODUCTION

With the progress in synthesizing a c-axis oriented single-domain bulk superconductor of a diameter exceeding 30mm [1-4], its application as a powerful permanent magnet has become more practical. Indeed, a superconducting permanent magnet has been already adopted in place of the Nd-Fe-B permanent magnet in the construction of a superconducting motor [5], magnetic separator [6] and magnetron sputtering [7-12]. In magnetron sputtering [7], a bulk superconductor cooled by a refrigerator down to about 40 K was magnetized and subsequently inserted below a target plate in order to confine the plasma immediately above it. The degree of plasma confinement has been evaluated by using a parameter $B_{//}^{max}$, magnetic field being defined on the target as that directed parallel to its surface and, hence, possessing a vanishing vertical or z-component [8-10].

The Nd-Fe-B magnet employed in a conventional magnetron sputtering can produce the $B_{//}^{max}$ value of only 0.05 Tesla on a non-magnetic target like Cu. We have reported that the $B_{//}^{max}$ value produced by the superconducting bulk magnet with 36 mm in diameter was 0.31-0.45 Tesla on the 3mm thick Cu target [7] and that its value was increased to 0.63 Tesla, when its diameter was increased to 60 mm [8-12]. Such a large $B_{//}^{max}$ enabled us to make the deposition of Cu in the Ar gas pressure range down to $1x10^{-3}$ Pa in comparison with the working pressure range above $1.5x10^{-1}$ Pa in a conventional one. Under such low Ar gas pressures, the mean free path of sputtered atom reaches several 10 cm. We could, therefore, deposit Cu onto the bottom of a circular via down to the diameter of 200 nm and the depth of 1.15 μm with its aspect ratio of about 6 in Si wafer.

In the present work, we report further progress in an increase in $B_{//}^{max}$ up to 1.0 and 1.2 Tesla on 3 and 1 mm thick Cu targets, respectively, and resulting Ar gas pressure dependence of deposition rates from Cu, Ni, Fe, Al and C targets. We also point out that the magnetron sputtering activated by a strong superconducting bulk magnet is particularly suited to the bottom coverage by Cu deposits onto a few 100 nanometer sized circular vias in Si wafer [11,12].

2. EXPERIMENTAL

The present 60 mmϕ c-axis oriented single domain Sm123 bulk superconductor was synthesized in the oxygen-controlled melt-growth (OCMG) method by adding 20 wt% Ag_2O and 0.5 wt% Pt to the powders mixed with the ratio Sm123:Sm211=3:1 [1,2].

The present magnetron sputtering apparatus is schematically illustrated in Fig.1 [7-12]. The bulk superconductor was mounted on a permendur yoke and cooled to 36 K on the cold stage of a Gifford-McMahon (G-M) refrigerator (AISIN SEIKI, TC101G). The cylindrical vacuum chamber connected to the G-M refrigerator can be

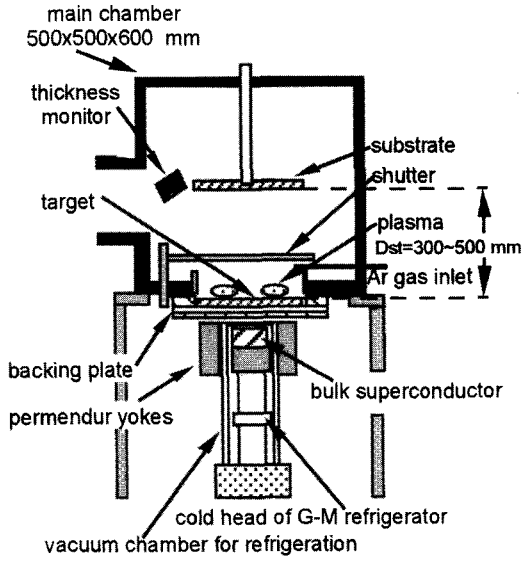

Fig.1 Schematic illustration of the present magnetron sputtering apparatus. The distance between the target surface and substrate is varied over 300-500 mm in the present work.

detached from the main chamber. The magnetization of the bulk superconductor was made by inserting the head of the vacuum chamber of 80 mm in outer diameter, inside which the bulk was mounted, into the bore of 100 mm in diameter of a 10 T superconducting solenoid magnet (Sumitomo Heavy Industries, HF10-100VHT). In the present experiment, maximum magnetic field of 6.6 T was applied to the superconducting bulk along the direction parallel to its c-axis at about 100 K well above its superconducting transition temperature of 94 K and reduced to zero after lowering the temperature to 42 K in the field cooling (FC) mode. The magnetized superconductor was further cooled to 36 K to prevent it from flux creeping.

After magnetization, the head of the vacuum chamber is inserted into an outer yoke ring made of permendur with 82 mm in inner diameter, 122 mm in outer diameter and 55 mm in height to allow flux lines evolving from the superconducting bulk magnet to be absorbed into the surrounding yokes as much as possible. The resulting flux density distribution above the

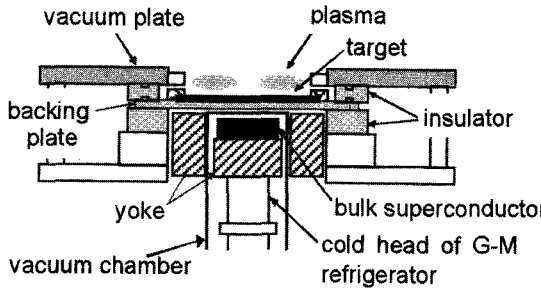

Fig.2 Schematic illustration of magnetron cathode in the present experiment.

surface of the vacuum chamber was measured by scanning a three-axial Hall sensor (AREPOC Ltd., AXIS-3). Then, the assembly is brought back to the bottom of the target in the main chamber, as shown in Fig.1. The magnetron cathode thus constructed is schematically illustrated in Fig.2. A distance between the surface of the superconductor and that of a target was 11 and 9 mm, when its thickness is 3 and 1 mm, respectively.

3. RESULTS AND DISCUSSION

3.1 Magnetic field distribution in the working space

After the construction of the superconducting bulk magnet sputtering apparatus, a main effort has been directed to an increase in $B_{//}^{max}$ and intensive efforts were made to synthesize a 60 mm diameter bulk superconductor as perfectly as possible and to further elaborate magnetization techniques. As mentioned in Introduction, the 36 mm-diameter Sm123-bulk superconductor was first employed. The value of $B_{//}^{max}$ on the 3 mm thick Cu target was 0.31 Tesla in the case of the apparatus shown in Fig.1 [7].

The value of $B_{//}^{max}$ was increased to 0.63 Tesla, i.e., about twice as large as that for the 36 mm bulk magnet, when it was replaced by a c-axis oriented single-domain Sm123 bulk superconductor of 60 mm in diameter (hereafter denoted as 60A) [8-12]. In the present experiment, another 60 mm-diameter Sm123 bulk superconductor (denoted as 60B) was installed after magnetization described above.

Figure 3 shows the magnetic field distribution

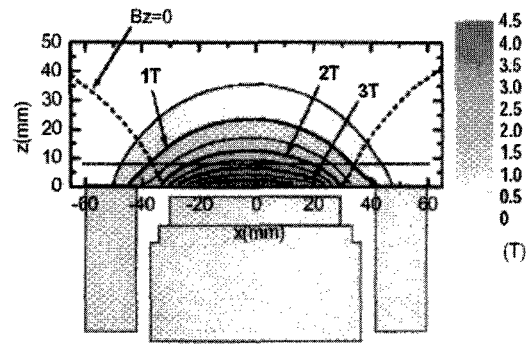

Fig.3. Distribution of magnetic fields produced by the Sm123 bulk superconductor magnetized in the FC mode under 6.6 T and 42 K. The bulk superconductor and surrounding yokes are shown. A horizontal line indicates the surface of the target of 3 mm in thickness. A dashed curve represents the field along which its z-component vanishes.

produced by the magnet 60B above the surface of the head of the vacuum chamber surrounded by the permendur yokes. The top surface of the vacuum chamber is positioned so as to coincide with the abscissa of the distribution map. One can see the position of the target surface, which is drawn as a horizontal line at z=8 mm.

It is seen from Fig.3 that the area, in which magnetic field exceeds 2 Tesla on the target, extends to 22 mm in radius from its center. Trapped fields further increased as compared with the magnet 60A, which produced 1.2 Tesla along the 22 mm-radius circle on the target [8-12].

The dashed curve in Fig.3 represents the line, along which the z-component of magnetic field is zero. The magnetic field, at which the dashed curve crosses the target surface, is referred to as $B_{//}^{max}$, as defined in Introduction. Its value is found to be 1.0 and 1.2 Tesla, when the non-magnetic Cu targets of 3 and 1 mm in thickness are employed, respectively.

3.2 Discharge current and deposition rate

Figure 4 shows the Ar gas pressure dependence of the discharge current under different target voltages for the magnet 60B in comparison with that for the 60A obtained under the same conditions: 3 mm thick Cu target and the throw distance D_{st}=300 mm [8-10]. The values of $B_{//}^{max}$ for the magnets 60A and 60B with 3 mm thick Cu target were 0.63 and 1.0 Tesla, respectively. One can clearly see an increase in the discharge current as a result of an increase in $B_{//}^{max}$. This is true, regardless of the magnitude of the Ar gas pressure and target voltage.

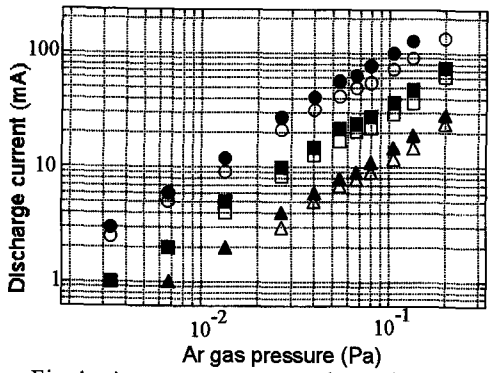

Fig.4 Ar gas pressure dependence of discharge current, when 3 mm thick Cu target was used. Open and solid symbols refer to the data taken with the magnets 60A and 60B, respectively. Triangles, squares and circles refer to the target voltages of 1, 2 and 6 kV, respectively.

The data on the deposition rate taken under the same conditions as Fig.4 are shown in Fig.5. Note that a conventional magnetron sputtering is by no means operated with a throw distance of 300-500 mm under Ar gas pressures down to 10^{-3} Pa. An adoption of the superconducting bulk magnet enabled us to carry out practical sputtering even under pressures down to at least 3.3 x 10^{-3} Pa. Under such high vacuum, the mean free path of sputtered atoms reaches a few 100 mm, which permitted us to employ a throw distance D_{st} longer than 300 mm. Thus, the deposition rate is not as high as that in a conventional sputtering. However, it should be noted that the deposition rate of 0.042 nm/s under the conditions D_{st}=300 mm, P=2.66 x 10^{-2} Pa, V=6 kV and $B_{//}^{max}$ = 1.0 T, corresponds to 2.3 nm/s or 1350 Å/min, if D_{st} is decreased to 40 mm like that in a conventional magnetron sputtering.

Similarly, we studied the behavior of both discharge current and deposition rate for 3 mm

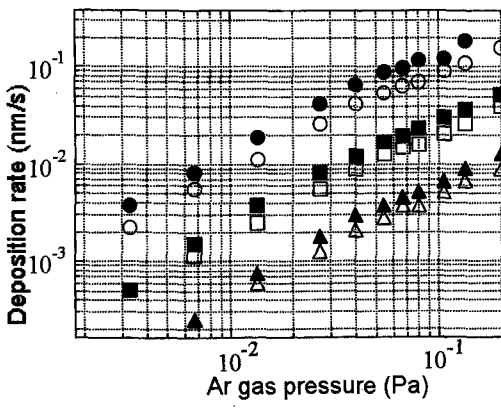

Fig.5 Ar gas pressure dependence of deposition rate, when 3 mm thick Cu target was used. Open and solid symbols refer to the data taken with the magnets 60A and 60B, respectively. Triangles, squares and circles refer to the target voltages of 1, 2 and 6 kV, respectively.

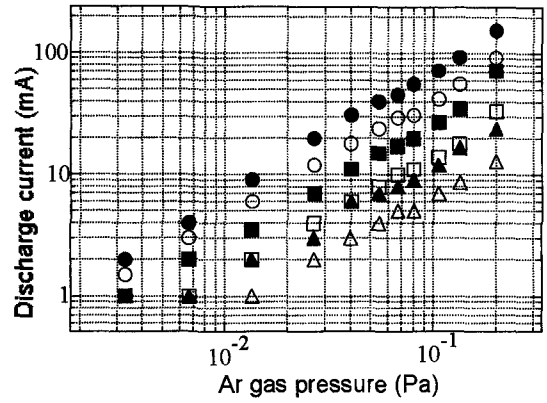

Fig.6 Ar gas pressure dependence of discharge current, when 3 mm thick Fe target was used. Open and solid symbols refer to the data taken with the magnets 60A and 60B, respectively. Triangles, squares and circles refer to the target voltages of 1, 2 and 6 kV, respectively.

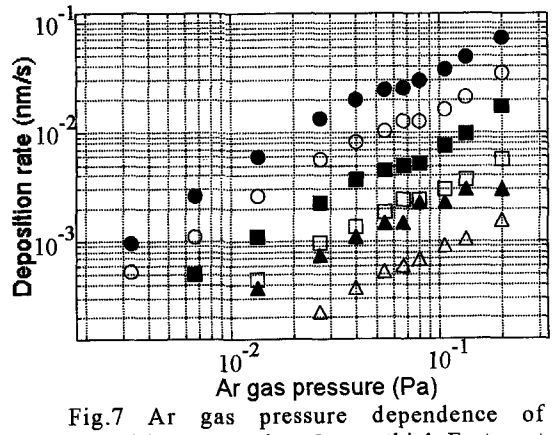

Fig.7 Ar gas pressure dependence of deposition rate, when 3 mm thick Fe target was used. Open and solid symbols refer to the data taken with the magnets 60A and 60B, respectively. Triangles, squares and circles refer to the target voltages of 1, 2 and 6 kV, respectively.

thick Fe target by varying Ar gas pressure under different target voltages. The results are shown in Figs.6 and 7, respectively. The discharge currents at D_{st}=300 mm, P=2.66x10^{-2} Pa and V=6 kV for Fe and Cu turned out to be 21 and 27 mA, respectively, the former reaching 78 % of the latter. This is worthwhile emphasizing. In a conventional magnetron sputtering, the discharging current for 3 mm thick Fe target is essentially nil because magnetic fluxes produced by the Nd-Fe-B magnet are mostly absorbed by magnetically soft Fe target. Therefore, we can safely say that a gain reaching 78 % is brought about as a result of a substantial increase in $B_{//}^{max}$ relative to that produced by the Nd-Fe-B magnet.

In contrast, the deposition rates for Fe and Cu are 0.0135 and 0.042 nm/s under the same condition as described above, the former being only 32% of the latter. The deposition rate has been often discussed in terms of the sputtering yield, which refers to the number of sputtered atoms per inert gas ion upon its bombardment onto a target. The sputtering yields of Cu and Fe are tabulated as 1.6 and 1.0, respectively, when Ar ions are accelerated to 400 eV [13]. This explains why the deposition rate for Fe is further lowered relative to that of Cu in spite of the possession of a comparable discharge current.

Figure 8 shows the Ar gas pressure dependence of

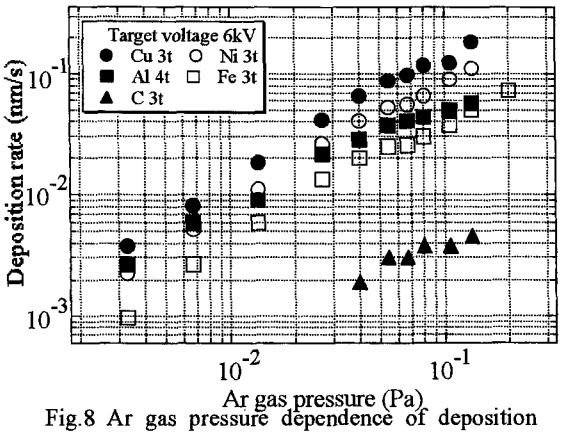

Fig.8 Ar gas pressure dependence of deposition rate for various elemental targets. The data were taken under the conditions Dst=300 mm, V=6 kV and $B_{//}^{max}$=1.0 Tesla.

the deposition rate from various elemental targets when the magnet 60B was employed. The deposition rate at a given Ar gas pressure decreases in the sequence of Cu, Ni, Al, Fe and C. This is consistent with the sputtering yields of 1.6, 1.2, 1.0, 0.8 and 0.1 for Cu, Ni, Fe, Al and C, respectively [13], except for the exchange in position between Al and Fe because of soft magnetic property of Fe mentioned above. But the difference in deposition rate between Fe and Al is reduced in the magnet 60B as compared with that in the magnet 60A [9].

Before ending this Section, we summarize in Fig.9 the $B_{//}^{max}$ dependence of the deposition rate for Cu obtained by using the magnets 60A and 60B. The deposition rate gradually increases on the logarithmic scale with increasing $B_{//}^{max}$ values throughout the Ar gas pressure range studied. At P=2.66x10^{-2} Pa or 2x10^{-4} Torr, for example, the deposition rate of Cu reaches 0.055 nm/s or 33 Å/min for the throw distance of 300 mm when $B_{//}^{max}$ is reached to 1.2 Tesla for 1 mm thick Cu

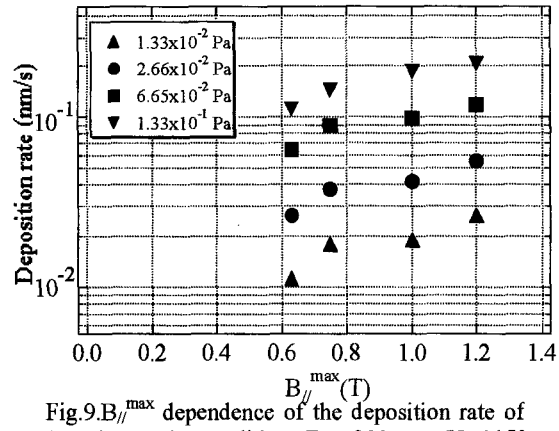

Fig.9.$B_{//}^{max}$ dependence of the deposition rate of Cu taken under conditions Dst=300 mm, V=6 kV with different Ar gas pressures.

target.

3.3 Bottom coverage by Cu deposit for 200 nm-class via holes in Si wafer

A conventional magnetron sputtering is generally unable to make a uniform Cu seed layer into the surface of a 200 nm-class narrow via hole in Si wafer. We believe a magnetron sputtering capable of extending D_{st} longer than 300 mm to be crucially important to achieve practical bottom coverage by Cu deposit for narrow via holes of this class. The present magnetron sputtering activated by a superconducting bulk magnet is, we believe, best suited for this purpose [11,12].

We employed Boro-Phospho Silicated Glass covered Si wafer, onto which via holes of 200-650 nm in diameter and 1.15 μm in depth were patterned and coated with 10 nm thick TiN as a barrier layer. Figure 10 shows the SEM micrographs of Cu film deposited into the hole of 650 nm in diameter and 1.15 μm in depth by using (a) the present sputtering apparatus shown in Fig.1 and (b) conventional one [14]. The substrate was positioned immediately above the target center and was not heated during sputtering.

The deposition in (a) was made under the conditions P=2.66 x 10^{-2} Pa, V=6kV, D_{st}=500 mm by using the magnet 60A in combination with 1 mm thick Cu target producing $B_{//}^{max}$=0.75 Tesla. The bottom coverage is defined as a ratio of the thickness of Cu film at the bottom of the hole over that on the substrate in percent [11,12]. The bottom coverage thus defined reached 100 %. It is important to note that Cu film in Fig.10 (a) was uniformly deposited everywhere including the sidewall of a deep hole without any overhang near the edge of the hole.

The micrograph (b) was taken with a conventional magnetron sputtering apparatus under conditions P=1.33 Pa, V= 400 V and D_{st} = 34 mm [12]. The bottom coverage turned out to be about 10 %. Small overhang is also seen at the edge of the hole. We consider the differences above to originate from that in the mean free path of sputtered Cu atoms in these two apparatus. As a matter of fact, the mean free path of sputtered Cu atom under the Ar gas pressure P=2.66x10^{-2} Pa is calculated to be about 250 mm and, thus, is scattered only fewer times before reaching the substrate. It is also true that the choice of a long throw distance in (a) could reduce the damage to the film due to less radiant heat of plasma.

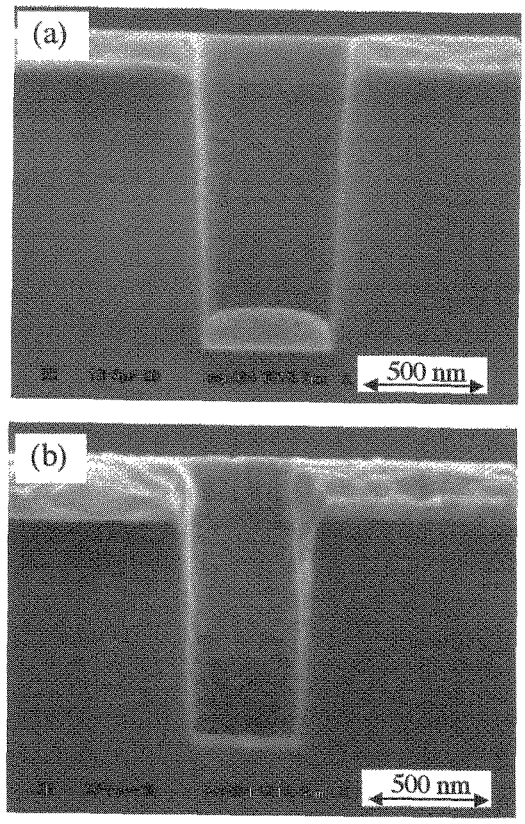

Fig.10. SEM micrograph of Cu film deposited into the hole of 650 nm in diameter and 1.15 μm in depth. The substrate was positioned straight above the target center: (a) deposited under the conditions P=2.66 x 10^{-2} Pa, V=6kV, D_{st} = 500 mm and $B_{//}^{max}$=0.75 Tesla, (b) deposited by using a conventional magnetron sputtering activated by the Nd-Fe-B magnet under conditions P=1.33 Pa, V=400 V and D_{st} = 34 mm.

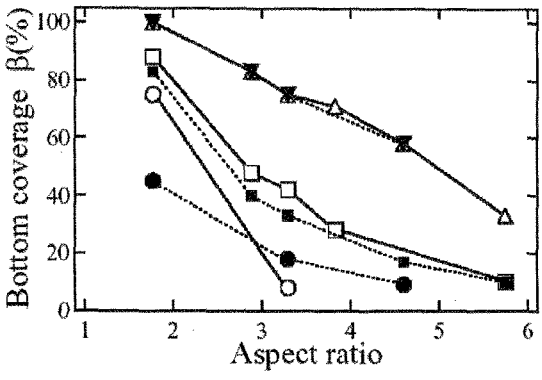

Fig.11. Aspect ratio dependence of the bottom coverage of Cu deposits under conditions P=2.66 x 10^{-2} Pa, V=6 kV and $B_{//}^{max}$=0.75 Tesla. Symbols refer to the data obtained with different throw distances: Dst=150mm (●, ○), Dst=300 mm (■, □) and Dst=500 mm (▼, △). Solid and open symbols represent the data obtained at the positions above the target center and the erosion ring, respectively.

Figure 11 shows the aspect ratio dependence of the bottom coverage under conditions P=2.66 x 10^{-2} Pa, V=6 kV and $B_{//}^{max}$=0.75 Tesla with three different D_{st} values [11,12]. Solid and dotted lines refer to the data obtained at positions straight above the target center and the erosion ring of 120 mm in diameter, respectively. A bottom coverage is increased and its position dependence becomes less significant with increasing D_{st}. For example, the deposition with D_{st}=500 mm resulted in a very high bottom coverage and allowed us to coat the hole with Cu film quite uniformly, regardless of the position on the surface of a substrate within at least 120 mm diameter, when a 150 mm diameter Cu target was used.

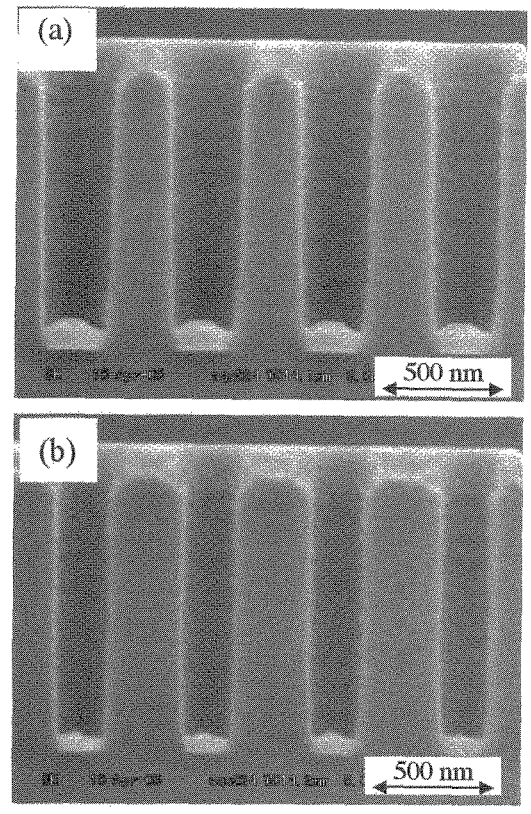

Fig.12 SEM micrographs of Cu film deposited into narrow holes of 1.15 μm in depth and (a) 350 nm and (b) 250 nm in diameter. The substrate is positioned straight above the target center under conditions P=2.66 x 10^{-2} Pa, V=6 kV, D_{st} =500 mm and $B_{//}^{max}$=0.75 Tesla.

Finally we show in Fig.12 the SEM micrographs of Cu film deposited into via holes of 350 nm and 250 nm in diameter and 1.15 μm in depth [12]. The substrate is positioned above the target center under conditions P=2.66 x 10^{-2} Pa, V=6 kV, D_{st}=500 mm and $B_{//}^{max}$=0.75 Tesla. A Cu film of 180 nm thick was deposited. The bottom coverage of the via hole of 350 nm (aspect ratio 3.29) and 250 nm (4.60) in diameter are found to be 75 and 58 %, respectively. A sidewall coverage of the via hole is also important for implanting Cu seed. The sputtered Cu film is deposited uniformly and continuously all over the sidewall, because magnetron sputtering with a long D_{st} can prevent the substrate from heating due to the radiant heat of plasma. This is also advantageous for the preparation of a Cu seed layer over other sputtering methods.

4. Conclusion

By using the magnetron sputtering apparatus activated by a superconducting bulk magnet, we could carry out practical sputtering under low pressures down to 10^{-3} Pa with D_{st}=300-500 mm. The deposition rate straight above the erosion ring from 3 mm thick Cu target is 0.042 nm/s (25 Å/min) with D_{st}=300 mm under 2.66×10^{-2} Pa and $B_{//}^{max}$=1.0 Tesla. Thanks to a substantial increase of $B_{//}^{max}$, the deposition of Fe from its 3 mm thick target can be successfully made with a discharge current comparable to that from Cu. We also proved that the present sputtering apparatus is capable of depositing Cu into a narrow 200-nm class via hole with a high aspect ratio. This is made possible as a result of a substantial increase in the mean free path of sputtered atoms in the Ar gas atmosphere. The bottom coverage is essentially position independent, when D_{st} is set at 500 mm in the Ar gas pressure $P=2.66\times10^{-2}$ Pa. Indeed, the bottom coverage of 58 % was realized for the via hole of 250 nm in diameter, regardless of positions over the Si substrate of 120 mm in diameter.

References

[1] H.Ikuta, A.Mase, Y.Yanagi, M.Yoshikawa, Y.Itoh, T.Oka and U.Mizutani, *Supercond. Sci. Technol.* **11**, 1345 (1998)

[2] H.Ikuta, T.Hosokawa, M.Yoshikawa and U.Mizutani, *Supercond. Sci. Technol.* **13** 1559 (2000)

[3] S. Nariki, N. Sakai and M. Murakami, *Physica C* **378-381** 631 (2002)

[4] G. Krabbes, Th. Hopfinger, C. Wende, P. Diko and G. Fuchs: *Supercond. Sci.Technol.* **15** 665 (2002)

[5] Y.Itoh, Y.Yanagi, M.Yoshikawa, T.Oka and U.Mizutani, *Japan.J.Appl.Phys.* **34** 5574 (1995)

[6] N. Saho, H. Isogami, T. Takagi and M. Morita, *IEEE Trans. on Applied Supercond.* **9** 398 (1999)

[7] U.Mizutani, T.Matsuda, Y.Yanagi, Y.Itoh, H.Ikuta and T.Oka, "*Processing of High-Temperature Superconducting Ceramic Transactions*", vol.140, edited by A.Goyal, W.Wong-Ng, M.Murakami and J.Driscoll, (2003) pp. 273-284

[8] T.Matsuda, S.Kashimoto, A.Imai, Y.Yanagi, Y.Itoh, H.Ikuta, U.Mizutani, K.Sakurai and H.Hazama, *Physica C* **392-396** 696 (2003)

[9] U.Mizutani, H.Hazama, T.Matsuda, Y.Yanagi, Y.Itoh, H.Ikuta, K.Sakurai and A.Imai, *Supercond.Sci.Technol.* **16** 1207 (2003)

[10] U.Mizutani, H. Hazama, T. Matsuda, Y. Yanagi, Y. Itoh, H. Ikuta, K. Sakurai and A. Imai, Proc. of 4th International Workshop on Processing and Applications of Superconducting (RE)BCO Large Grain Materials", Jena, Germany (2003)

[11] H. Hazama, T. Matsuda, U. Mizutani, H. Ikuta, Y. Yanagi, Y. Itoh, K. Sakurai, A. Sekiguchi and A. Imai, submitted to *Japan.J.Appl.Phys.* (2003)

[12] H. Hazama, A. Imai, T. Matsuda, U. Mizutani, H. Ikuta, Y. Yanagi, Y. Itoh, K. Sakurai, A. Sekiguchi and T. Yamazaki, presented at ADMETA (2003)

[13] N.Laegreid,G.K.Wehner:J.Appl.Phys.**32** 365 (1961)

[14] T.Yamazaki, Japan.J.Appl.Phys. **29**, 1304-1309 (1990)

(Received October 13, 2003; Accepted March 5, 2004)